Electric Power Systems Research xxx (2016) xxx–xxx

Contents lists available at ScienceDirect

Electric Power Systems Research

journal homepage: www.elsevier.com/locate/epsr

Advanced fault location strategy for modern power distribution systems based on phase and sequence components and the minimum fault reactance concept

Cristian Grajales-Espinal, Juan Mora-Flórez*, Sandra Pérez-Londoño

Electrical Engineering Program, Universidad Tecnológica de Pereira, Pereira, Colombia

ARTICLE INFO

Article history:
Received 30 June 2015
Received in revised form
30 September 2015
Accepted 9 April 2016
Available online xxx

Keywords:
Distributed generation
Fault location
Minimum fault reactance
Power distribution systems
Sequence networks
Shunt faults

ABSTRACT

A generalized strategy for fault location in modern power distribution systems, which normally include distributed generation, is presented in this paper. The fault location method considers the phase and sequence network parameters and voltage and current measurements at the main substation and at the distributed generators, in pre-fault and fault steady states. The fault distance is estimated from the analysis of all section lines, which is required to determine if the fault is located in a radial or non-radial zone of the power distribution feeder; next, a specific equation is used to determine the exact location. The proposed methodology is validated in the IEEE 34-node test power system, where single-phase to ground, phase-to-phase and three-phase faults were tested, considering 51 different and optimally determined operational conditions. The proposed method has range of estimation errors from −2.8% to 3.2%.

1. Introduction

During the past few years, a growing interest in installing small generation units along distribution systems, which are known as distributed generators (DGs), was experienced. These DGs are used to take advantage of primary energy resources as wind and solar radiation, among others, and also to improve voltage profiles and to reduce constrains of transmission and distribution systems [1]. The presence of DGs implies that new studies aimed to analyze their effects for reliability, losses, voltage regulation, relay coordination and fault location, among others [2–4].

Additionally, the DG presence causes relevant operational changes in power distribution systems, such as non-radial supplied feeders, which has a direct consequence in the performance of the impedance-based fault locators. Although several methods have been proposed for fault location in power distribution systems, most of them are not well suited when DG is presented [5]. Additionally, most of the methods proposed for fault location in power distribution systems with DG do not consider the different operating conditions, and then these are tested normally at the rated or well-known conditions [6–15]. This situation does not offer the possibility of an adequate evaluation of the fault locator performance.

At the previous research, a fault location methodology aimed to consider only single-phase to ground faults, based on sequence components as proposed in [11]. This uses information of the circuit topology and measurements of voltage and current at the main substation and the DG substation; however, this methodology neglects line capacitance, and phase-to-phase and three-phase faults are not considered. Additionally, a criterion for the selection of the fault distance was not defined in the case of multiple solutions. On the other hand, a method for three-phase to ground fault location based on the estimation of the positive sequence impedance is proposed in [10]; however, line capacitance and load variations are not considered and the method is not generalized for single-phase or phase-to-phase faults. A methodology based on the system phase-components is presented in [12], which considers an unbalanced power distribution system, but it is limited to three-phase to ground faults and its efficiency is not tested considering load variations. In [13], there is an interesting approach, which considers the line shunt admittance matrix at the power system representation. The authors consider any fault type but tests are performed under the rated operational condition of the power system. An additional approach is proposed in [14] and is aimed to discuss a ranking of the available fault location methods that take into account

* Corresponding author. Tel.: +57 300 678 5932; fax: +57 6 3137122.
E-mail addresses: cdgrajales@utp.edu.co (C. Grajales-Espinal), jjmora@utp.edu.co (J. Mora-Flórez), saperez@utp.edu.co (S. Pérez-Londoño).

http://dx.doi.org/10.1016/j.epsr.2016.04.008
0378-7796/

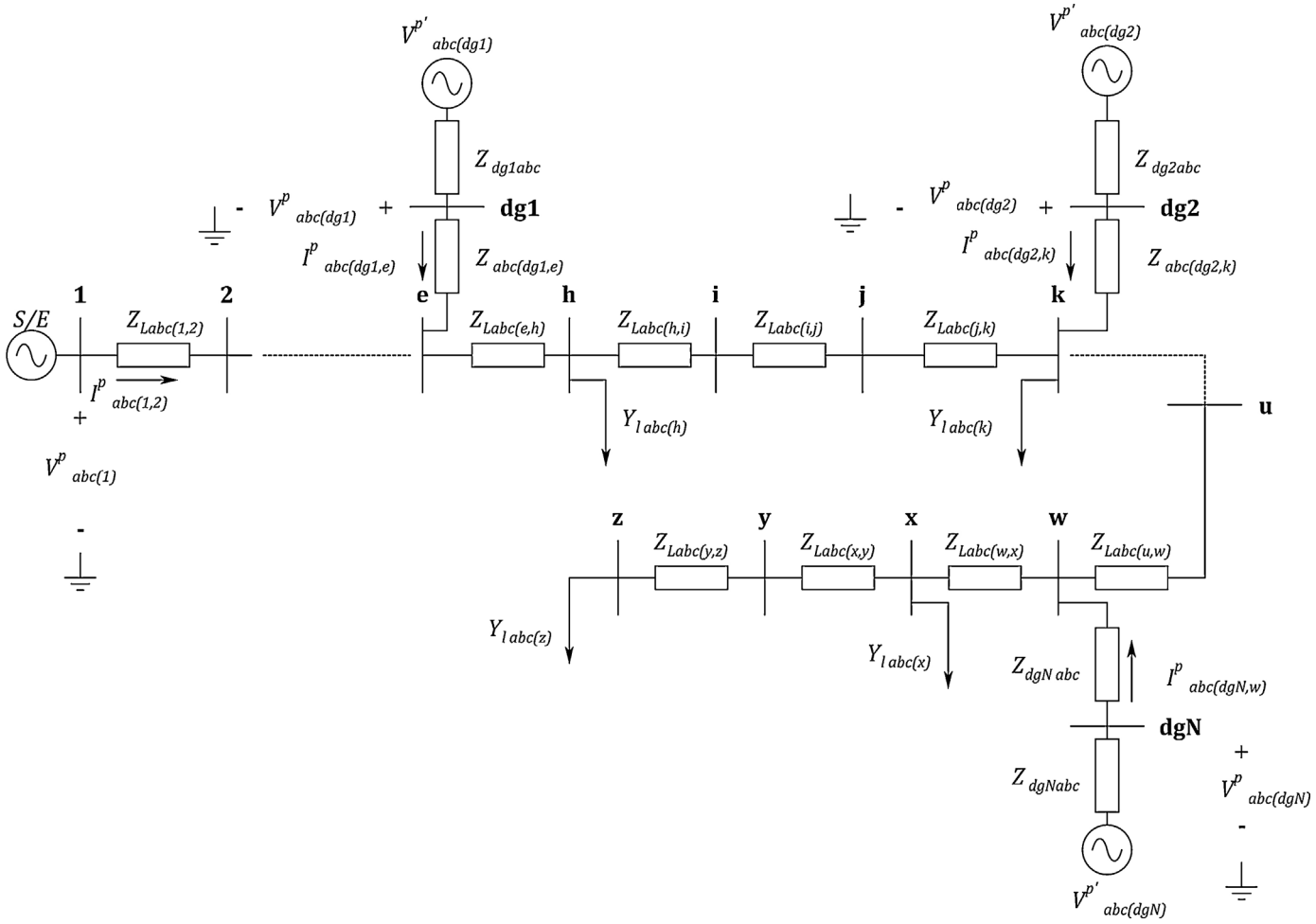

Fig. 1. Simplified power distribution system with *N* distributed generators.

application requirements and modelling limitations and uncertainties. This uses qualitative and quantitative analysis, and as a result, two impedance-based approaches were selected and tested in detail, considering the rated operating condition. In [15], authors propose a solution that eliminates or reduces iterative procedures applicable to all types of faults. The proposed methods are based on the bus impedance matrix. This paper neglects the shunt capacitances of feeders in the simulation model. Rated conditions of the power system are considered in tests. Finally in [16], a letter briefly presents a method for locating a fault in distribution systems using synchrophasor measurements. Using voltage and current phasor measurements at substations and/or feeder heads, candidate fault locations are identified by iterating every possible line segment. The tests, considering the rated operating condition, are commented on, where the solution is obtained by using a not described impedance-based method.

This paper is aimed to present a general methodology for fault location in power distribution systems with DG, considering the robustness of the method in the case of uncertainties associated to load variations and different DG penetration levels, and surpassing some of the main problems of the above-mentioned approaches. The method here proposed is oriented to use only measurements at the fundamental frequency component of current and voltage at the main power substation and at the DGs and the series and shunt parameters of a long line equivalent. The information required for the fault location are the fundamental phasors, during steady states of pre-fault and fault, for voltages and currents; these are available at protective relays, digital fault recorders and power quality metres. The measurements have to be synchronized and the fault time is normally used as the time reference. This makes the fault locator useful for most of the actual power distribution networks.

With regard to the contents, in Section 2, this paper presents the theoretical foundation of the proposed approach. The developed algorithm for the method implementation is completely described in Section 3. Tests, results and discussion are included in Section 4, and the most relevant conclusions of the research are summarized in Section 5.

2. Proposed fault location method

The proposed method is defined by using the simplified power distribution system as presented in Fig. 1, which consists of a main source (S/S), *N* distributed generators and several tapped loads. The power system upstream node **w** represents the non-radial circuit zones, where the fault current is supplied from the sending and the receiving-end nodes of the faulted line section. On the other hand, the power system downstream node **w** corresponds to a radial circuit zone, where the fault current is supplied only from the sending-end node of the faulted line section. Here, the proposed methodology considers more than one DG, laterals, tapped loads and different line configurations.

Please cite this article in press as: C. Grajales-Espinal, et al., Advanced fault location strategy for modern power distribution systems based on phase and sequence components and the minimum fault reactance concept, Electr. Power Syst. Res. (2016), http://dx.doi.org/10.1016/j.epsr.2016.04.008

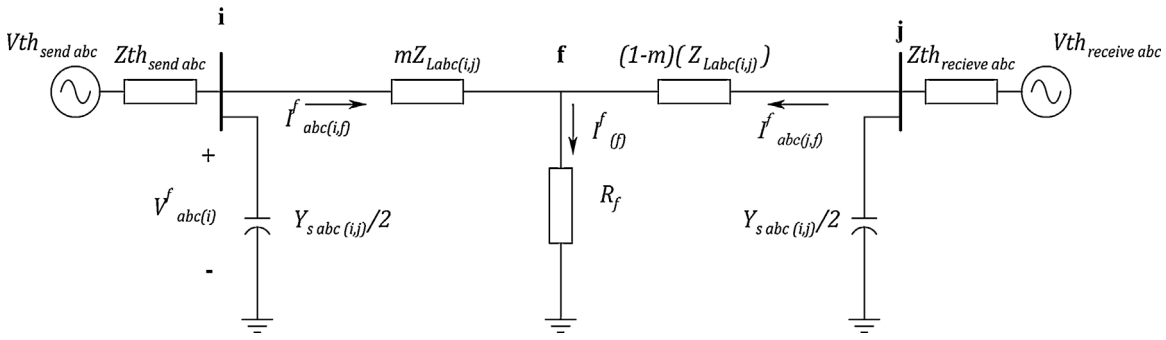

Fig. 2. Faulted line section of a non-radial power system zone under study.

The variables in Fig. 1 are described as the following:

$Z_{Labc(i,j)}$ phase impedance of the line section from node **i** to node **j**.
Z_{dgNabc} phase internal impedance of the distributed generator *N* (DGN).
$Y_{labc(i)}$ phase load admittance matrix connected at node *i*.
$V^{p}_{abc(i)}$ phase voltages in pre-fault steady state at node *i*.
$I^{p}_{abc(i,j)}$ phase currents in pre-fault steady state, flowing from node *i* to node *j*.
$V^{p}_{abc(dgN)}$ phase voltages in pre-fault steady state measured at node **dgN**.
$I^{p}_{abc(dgN,j)}$ phase currents in pre-fault steady state, flowing from node **dgN** to node *j*.
$V^{p'}_{abc(dgN)}$ internal phase voltages in pre-fault steady state of the *N* DG.

The fault current varies depending on the fault location and also the location of the DGs. Then, the proposed methodology considers two scenarios for the determination of the fault distance: faults at radial and non-radial power system zones.

2.1. Fault location analysis for non-radial faulted zones of a power distribution system

The proposed analysis for faults in non-radial zones is based on the reduced power system in Fig. 2, which depicts a faulted line section where the fault current is supplied from both ends.

The new variables in Fig. 2 are next described as follows:

$Zth_{send\ abc}$ phase Thevenin impedance as seen from the sending-end node.
$Zth_{receive\ abc}$ phase Thevenin impedance as seen from the receiving-end node.
$Y_{s\ abc(i,j)}$ shunt admittance matrix of the line section from node **i** to node **j**.
$Vth_{send\ abc}$ phase Thevenin voltages at the sending-end node.
$Vth_{receive\ abc}$ phase Thevenin voltages at the receiving-end node.
$V^{f}_{abc(i)}$ phase voltages in fault steady state, at node **i**.
$I^{f}_{abc(i,f)}$ phase currents in fault steady state, flowing from node **i** to node **f**.
R_f fault resistance.
m per unit fault distance based on the line section length from node **i** to node **j**.

The Thevenin equivalents at the receiving-end and the sending-end nodes are used to represent the circuit downstream node **j** and the circuit upstream node **i,** respectively, as is proposed in [11] to consider the effect of the DG. The application of the here proposed methodology is extended for *N* distributed generators as is next presented.

2.1.1. Step 1. Calculate the internal voltages of DGs at the pre-fault steady state

The internal voltage at the DG during pre-fault steady state is obtained from the measurements of voltage and current at node **dgN** in Fig. 1 ($V^{p}_{abc(dgN)}$, $I^{p}_{abc(dgN,w)}$) and Z_{dgNabc}, through Eq. (1).

$$V^{p'}_{abc(dgN)} = V^{p}_{abc(dgN)} + Z_{dgNabc} I^{p}_{abc(dgN,w)} \quad (1)$$

2.1.2. Step 2. Determine the Thevenin voltage at node j

The Thevenin voltage at node *j* is calculated using Fig. 3a, which represents the subsystem downstream node **j** of the power system in Fig. 1. The superposition principle is used to consider all the DGs downstream node **j**; it states that the voltage in any node of the power system, having more than one independent voltage source, is equal to the sum of the responses caused by each independent source acting individually, where all the other independent sources are set to zero.

In the case when considering only the *N* distributed generator, the impedance of the modified power system presented in Fig. 3a is lumped at **dgN** node. Next, the internal voltage and impedance of DGN is used to determine the current supplied to the power system, and the voltage at node **j** is then estimated. This procedure is repeated for each DG downstream node **j**. Finally, the Thevenin voltage at node *j* is calculated by the addition of each contribution of the different DGs downstream node *j*, through Eq. (2).

$$Vth_{receive\ abc} = \sum_{s=1}^{dw} Vth_{receive\ abc\ s} \quad (2)$$

where, *dw* is the number of DGs downstream of the receiving-end node (node **j**) and $Vth_{receive\ abc\ s}$ is the phase voltage calculated at node **j** considering each independent source *s*, acting individually.

2.1.3. Step 3. Estimate the Thevenin impedance as seen from node j

The Thevenin impedance downstream of the node **j** is calculated using Fig. 3a. The voltage sources that represent the DGs are set to zero, and finally the impedance of the modified circuit is lumped at node **j**.

2.1.4. Step 4. Determine the Thevenin equivalent upstream node i

Finally, the Thevenin equivalent that represents the power system upstream to node **i** is obtained from Fig. 3b. The estimation of this equivalent follows the same methodology as proposed for the power system downstream the node **j**, as described in the previous

Please cite this article in press as: C. Grajales-Espinal, et al., Advanced fault location strategy for modern power distribution systems based on phase and sequence components and the minimum fault reactance concept, Electr. Power Syst. Res. (2016), http://dx.doi.org/10.1016/j.epsr.2016.04.008

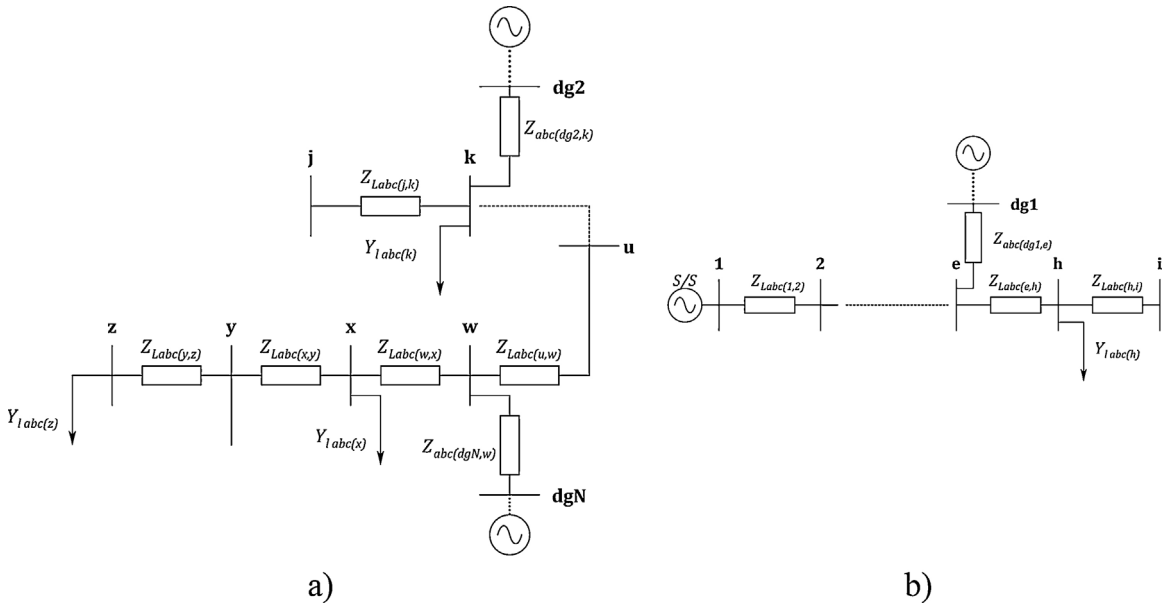

Fig. 3. Subsystems of the power distribution system in Fig. 1 which contains DGs: (a) downstream node *q*; and (b) upstream node *p*.

steps, and then the main substation is considered as another DG. Eq. (3) helps to obtain the voltage for the sending-end node (node **i**).

$$Vth_{send\,abc} = \sum_{s=1}^{up} Vth_{send\,abc\,s} \tag{3}$$

where, *up* is the number of DGs upstream of the sending-end node (node **i**), including the main substation and $Vth_{send\,abc}$ is the phase voltage calculated at node **i** by each independent source acting individually.

The Thevenin impedance upstream of the node **i** is calculated using Fig. 3b. The voltage sources are set to zero, and finally the impedance of the modified circuit is lumped at node **i**.

2.1.5. Step 5. Estimate the sequence equivalent of the faulted section

From the faulted section representation in Fig. 2, the sequence component transformation is applied. Next, the sequence networks are interconnected according to the fault type. Fig. 4 shows the equivalent sequence network for the faulted line section of a non-radial zone of the analyzed power system.

The variables in Fig. 4 are described as the following:

$Z_{l\,012(i,j)}$ sequence impedance of the line from node **i** to node **j**.
$Zth_{send\,012}$ sequence Thevenin impedance seen from the sending-end node **i**.
$Zth_{receive\,012}$ sequence Thevenin impedance seen from the receiving-end node **j**.

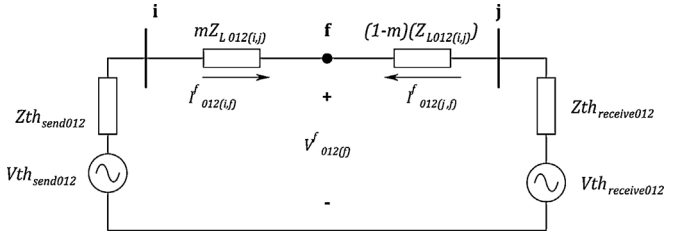

Fig. 4. Equivalent sequence network for faulted line section of non-radial power system zone.

$Vth_{send\,012}$ sequence Thevenin voltages at the sending-end node **i**.
$Vth_{receive\,012}$ sequence Thevenin voltages at the receiving-end node **j**.
$V^f_{012(f)}$ sequence voltages in fault steady state, at the faulted node **f**.
$I^f_{012(p,f)}$ sequence currents in fault steady state, flowing from node **p** to node **f**.
$I^f_{012(q,f)}$ sequence currents in fault steady state, flowing from node **q** to node **f**.

The sequence network interconnection for a single-phase to ground, two-phase and three-phase faults, is performed according to as suggested in [17].

2.1.6. Step 6. Calculate the fault location

The application of Kirchhoff voltage law only at the positive sequence network, as the one shown in Fig. 4, helps to obtain (4) and (5).

$$V^f_{1(f)} = Vth_{send\,1} - Zth_{send\,1} I^f_{1(i,f)} - mZ_{L1(i,j)} I^f_{1(i,f)} \tag{4}$$

$$V^f_{1(f)} = Vth_{receive\,1} - (Zth_{receive\,1} + Z_{L1(i,j)} - mZ_{L1(i,j)}) I^f_{1(i,j)} \tag{5}$$

The fault distance *m* in per unit is obtained from (4) and (5), as shown in (6).

$$m = \frac{Vth_{send\,1} - Zth_{send\,1} I^f_{1(i,f)} - Vth_{receive\,1} + (Zth_{receive\,1} + Z_{L1(i,j)}) I^f_{1(j,f)}}{Z_{L1(i,j)} (I^f_{1(j,f)} + I^f_{1(i,f)})} \tag{6}$$

Eq. (6) is the general expression to determine the fault distance at the non-radial zone of the power system, avoiding the determination of the fault type and resistance.

In the case of faults not located at the analyzed line section **i**–**j** (i.e. $m > 1$), all the previous procedure from step 2 to step 6 is repeated, and a new estimation of the fault distance is performed for the next section between nodes **j** and **k**.

The previously defined procedure is applied in all section lines of the non-radial faulted zones, until a value lower than 1.0 of the

Please cite this article in press as: C. Grajales-Espinal, et al., Advanced fault location strategy for modern power distribution systems based on phase and sequence components and the minimum fault reactance concept, Electr. Power Syst. Res. (2016), http://dx.doi.org/10.1016/j.epsr.2016.04.008

fault distance in per unit (m) of the analyzed section is reached. The line section where m has a value lower than 1.0 is selected as the faulted section, and the fault distance is obtained as the product of m and the line section length.

2.2. Fault location analysis for radial faulted zones of a power distribution system

For faults in a radial zone, the algorithm for fault distance estimation is based on the approach proposed in [11,18]. In this case, the fault location method is proposed using the line section representation given at Fig. 2, but the source at the receiving end does not exist. To analyze this case, the faulted line section is supposed in a radial section downstream of all the power generators. Section between **w** and **x** nodes of the power system in Fig. 1 is selected to present the proposed approach.

The effect of currents supplied by DGs has to be considered before the estimation of the voltage and current feeding the line section under study. Considering the power distribution system in Fig. 1, node **w** represents a common connection point, i.e., a node where a new DG is connected. From this point downwards, the distribution feeder has a radial structure, where the current flowing from **w** to **f** is the contribution of all the DGs, updated from their respective substations to node **w**, and is proposed in (7).

$$I^f_{abc(w,f)} = I^f_{abcS/S(w,f)} + \sum_{i=1}^{N} I_{abc\,DG\,i(w,f)} \tag{7}$$

where,

$I^f_{abc(w,f)}$ phase current that flows from node **w** to node **f**.
$I^f_{abcS/S(w,f)}$ phase current supplied by the main substation, updated to node **w**.
$I_{abcDG\,i(w,f)}$ current supplied by the i DG unit, updated to node **w**.

For faults at radial zones of the power distribution feeder, it is necessary to identify the fault type, as each fault requires a different set of equations to estimate the fault distance. The algorithm proposed by Das is used for fault type identification [19]. The fault distance estimation is based on a sequence network interconnection analysis, where (8) summarizes the calculation of the fault distance (m) for all fault types [18].

$$Bm^2 + Cm + D = R_f A \tag{8}$$

Coefficients A, B, C and D are calculated according to fault type, as is shown next.

2.2.1. Step 1. Determination of coefficients according to the fault type

According to the fault type, the coefficients in Eq. (8) are obtained as presented in the following:

a. Single-phase to ground faults

The coefficients of (8) in the case of single-phase to ground faults are given in (9).

$$\begin{aligned}
A &= 3(Z_{L1(w,x)}I^f_{1(w,f)} + Z_{C1}I^f_{1(w,f)} - V^f_{1(w)})\\
B &= Z_{L0(w,x)}Z_{L1(w,x)}I^f_{0(w,f)} + Z^2_{L1(w,x)}I^f_{1(w,f)} + Z_{L1(w,x)}Z_{L2(w,x)}I^f_{2(w,f)}\\
C &= -Z_{L0(w,x)}Z_{L1(w,x)}I^f_{0(w,f)} - Z^2_{L1(w,x)}I^f_{1(w)} - Z_{L2(w,x)}Z_{L1(w,x)}I^2_{2(w,f)}\\
&\quad -Z_{L1(w,x)}V^f_{0(w)} - Z_{L1(w,x)}V^f_{1(w)} - Z_{L1(w,x)}V^f_{2(w)}\\
&\quad -Z_{L0(w,x)}I^f_{0(w,f)}Z_{C1} - Z_{L1(w,x)}I^f_{1(w,f)}Z_{C1} - Z_{L2(w,x)}I^f_{2(w,f)}Z_{C1}\\
D &= Z_{L1(w,x)}V^f_{0(w)} + Z_{L1(w,x)}V^f_{1(w)} + Z_{L1(w,x)}V_{2(w)}\\
&\quad +Z_{C1}V^f_{0(w)} + Z_{C1}V^f_{1(w)} + Z_{C1}V^f_{2(w)}
\end{aligned} \tag{9}$$

where, Z_{C012} is the sequence impedance of the power system downstream the receiving-end node (node **x**) and lumped at that node.

b. Phase-to-phase faults

The coefficients given in Eq. (8), in the case of phase-to-phase faults, are presented in (10).

$$\begin{aligned}
A &= V^f_{1(w)} - Z_{L1(w,x)}I^f_{1(w,f)} - Z_{c1}I^f_{1(w,f)}\\
B &= Z_{L1(w,x)}Z_{L2(w,x)}I^f_{2(w,f)} - Z^2_{L1(w,x)}I^f_{1(w,f)}\\
C &= Z_{L1(w,x)}V^f_{1(w)} - Z_{L1(w,x)}V^f_{2(w)} - Z_{L2(w,x)}Z_{L1(w,x)}I^f_{2(w,f)}\\
&\quad +Z_{L1(w,x)}I^f_{1(w,f)}Z_{C1} - Z_{L2(w,x)}I^f_{2(w,f)}Z_{C1} + Z^2_{L1(w,x)}I^f_{1(w,f)}\\
D &= Z_{L1(w,x)}V^f_{2(w)} + Z_{C1}V^f_{2(w)} - Z_{L1(w,x)}V^f_{1(w)} - Z_{C1}V^f_{1(w)}
\end{aligned} \tag{10}$$

c. Three-phase faults

The coefficients of (8) in the case of three-phase faults are shown in (11).

$$\begin{aligned}
A &= Z_{L1(w,x)}I^f_{1(w,f)} + Z_{c1}I^f_{1(w,f)} - V^f_{1(w)}\\
B &= Z^2_{L1(w,x)}I^f_{1(w,f)}\\
C &= -Z_{L1(w,x)}V^f_{1(w)} - Z^2_{L1(w,x)}I^f_{1(w,f)} - Z_{L1(w,x)}I^f_{1(w,f)}Z_{C1}\\
D &= Z_{L1(w,x)}V^f_{1(w)} + Z_{C1}V^f_{1(w)}
\end{aligned} \tag{11}$$

2.2.2. Step 2. Proposed criterion to determine the best estimated distance

The proposed method uses a quadratic equation to determine the fault distance, which leads to two possible solutions; however, an adequate criterion for the selection of the best solution was not previously defined in the original paper presented in [18], in the case of radial zones. A proposed method for this decision is established as is presented in the following:

a. Estimate all of the possible values of m, by calculating all of the possible fault distances along the power distribution feeders.

The complete analysis of the power distribution system considers the update of the voltages and currents through the entire radial power system, using the expressions (12) and (13), respectively. These expressions are used to obtain the voltage at node **x** and the current flowing from **x** to **y**, using the voltage at node **w** and the current flowing from node **w** to node **x**.

$$V^f_{abc(x)} = V^f_{abc(w)} - Z_{Labc(w,x)}I^f_{abc(w,x)} \tag{12}$$

$$I^f_{abc(x,y)} = I^f_{abc(w,x)} - \left(Y_{l\,abc(x)} + \frac{Y_{s\,abc(w,x)}}{2} + \frac{Y_{s\,abc(x,y)}}{2}\right) V^f_{abc(x)} \tag{13}$$

Please cite this article in press as: C. Grajales-Espinal, et al., Advanced fault location strategy for modern power distribution systems based on phase and sequence components and the minimum fault reactance concept, Electr. Power Syst. Res. (2016), http://dx.doi.org/10.1016/j.epsr.2016.04.008

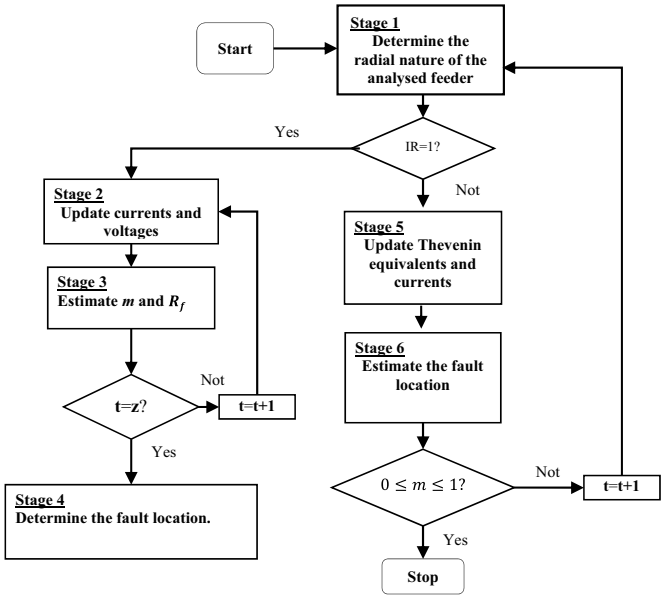

Fig. 5. Algorithm for the estimation of the distance to a faulted node.

In this way, all line sections of the radial power system (downstream node **w** of the power system in Fig. 1) are analyzed and several values of m are estimated.

b. Determine those values of m, which are at the interval [0,1].
c. For each value of m, estimate the corresponding fault reactance (X_f).
d. Determine, for the values of m previously estimated, which is the minimum fault reactance and select it as the fault location. This concept is useful, because in most of the cases the fault impedance is composed by a large resistive component and a very small reactive component [20].

3. Proposed generalization of the fault location algorithm

The proposed algorithm to estimate the distance to the faulted node, considering the power system in Fig. 1, is described in stages and depicted in Fig. 5.

3.1. Stage 1. Determine the radial nature of the analyzed feeder

Determine if the line section under study is in a radial zone or in a non-radial zone of the power distribution feeder. If the line section is in a radial zone (IR = 1), go to stage 2; otherwise, go to stage 5 (IR = 0). The analyzed line section is represented by counter t which is initialized as $t = 1$

3.2. Stage 2. Update currents and voltages at the analyzed section line

Voltages and currents are updated to the line section under study using Eqs. (12) and (13), respectively, taking into account the line capacitive effect and the load variations. The load variations are considered by using a load correction factor β, as presented in (14).

$$\beta = \frac{I'^{p}_{abc}}{I'^{p}_{abc\text{-}rated}} \tag{14}$$

In (14), $I'^{p}_{abc\text{-}rated}$ are the phase pre-fault average currents under rated conditions and I'^{p}_{abc} are the phase pre-fault average currents measured at the analyzed load scenario. The β factor is multiplied to each load, in order to adjust load values at the operational condition of the faulted power distribution system.

3.3. Stage 3. Estimate m and R_f

Calculate the values of the fault distance and the fault resistance using Eq. (8). The solution is determined considering the fault type through Eqs. (9), (10) or (11), for single-phase, phase-to-phase or three-phase faults, respectively. This step considers the estimation in all section lines at the analyzed radial feeder.

3.4. Stage 4. Determine the fault location

Evaluate the necessary conditions for the selection of the most adequate fault location, considering the minimum fault reactance, as is proposed in Section 2.2.2.

Finally, Stages 5 and 6 are applied for fault location in non-radial zones of the distribution feeder, as described in the following:

3.5. Stage 5. Estimate the Thevenin equivalent

Obtain the Thevenin equivalent of the feeder downstream the receiving-end node and upstream the sending-end node, based on the proposed methodology presented in Section 2.1 and by using Eqs. (1)–(3). Load variations must be taken into account during the Thevenin impedance estimation using Eq. (14), to mitigate the effect to load variation.

3.6. Stage 6. Estimate the fault distance m

Estimate fault location using (6) and check if m is between 0 and 1. In this case, the fault is located at the line section under study. Otherwise, update the Thevenin equivalent of the sending-end node and the receiving-end node and go to Stage 1.

4. Tests and result analysis

4.1. Test system and scenarios

The proposed fault location method is validated at the 24.9 kV IEEE 34-node test system. This system contains unbalanced loads, single-phase and three-phase feeders, line capacitive effects and different length line sections, conductors and configurations. The power system is modified, in order to include two distributed generators at nodes 840 and 856 [21].

To validate the proposed approach, fault simulation in different nodes of the analyzed power system, considering single-phase to ground, phase-to-phase and three-phase faults for fault resistances between 0 Ω and 40 Ω, is performed. According to several utility reported studies, most of the faults in power distribution systems have resistance values lower than 40 Ω [22].

For testing purposes, the rated condition plus 50 optimally determined operating conditions were selected, using the Latin Hypercube optimal sampling method [23]. Each operating condition is obtained from a range between 10% and 150% of the rated load, for all of the power system loads, and from 0% to 50% of the DG penetration.

Considering the previous that were exposed, a total of 9945 faults were used in the testing process}.

4.2. Results and analysis

The method performance is determined by using Eq. (19).

$$\textit{Absolute error} \quad [\%] = \frac{D_{Real} - D_{Calculated}}{L_{Total}} \times 100 \tag{15}$$

Please cite this article in press as: C. Grajales-Espinal, et al., Advanced fault location strategy for modern power distribution systems based on phase and sequence components and the minimum fault reactance concept, Electr. Power Syst. Res. (2016), http://dx.doi.org/10.1016/j.epsr.2016.04.008

where, D_{Real} is the real distance to the faulted node, $D_{Calculated}$ is the distance calculated by the fault location method, and L_{Total} is the total length of the analyzed feeder.

4.2.1. Estimation of the fault locator performance under rated conditions

Results obtained under rated conditions for two penetration levels of DG (10% and 35%) and for the three fault types are shown in Figs. 6–8. At these figures, different fault resistances, are considered (0.05, 10, 20, 30 and 40 Ω).

(a) Single-phase to ground faults

From Fig. 6a and b, it is possible to conclude that the method performance is satisfactory for single-phase to ground faults, because the highest error for all the DG scenarios is −2.8%, in the case of a fault resistance of 40 Ω.

The errors presented are caused by the power system unbalance, single- and double-phase laterals, not well considered in the sequence-based component methods. Additionally, it is clear from Fig. 6 that the error increases as fault resistance rises, and an overestimation of the fault location is then obtained.

(b) Phase-to-phase faults

The results in the case of phase-to-phase faults are presented in Fig. 7. Based on these results, it is noticed that the proposed method is also suitable for phase-to-phase fault location. In this case, the highest error is 3.8%, and similarly to the single-phase to ground fault case, these errors are due to approximations related to sequence network coupling. Additionally, the errors on fault location are higher than these obtained in the case of single-phase faults, and the underestimation of the fault location is presented. Finally, the error increases for high values of fault resistance.

(c) Three-phase faults

From the results depicted in Fig. 8, lower estimation errors occur when higher levels of DG are considered. In this case, the maximum estimation error considering a DG penetration level of 10% is 1.4%; however, for a DG penetration level of 35%, the highest estimation error is 1.1%. Nevertheless, these differences are irrelevant and have no effect on the performance and then errors are below 1.4%.

4.2.2. Estimation of the fault locator performance under non-rated load conditions

In this case, 50 different operating conditions (9750 faults) were used to analyze the performance of the fault location method,

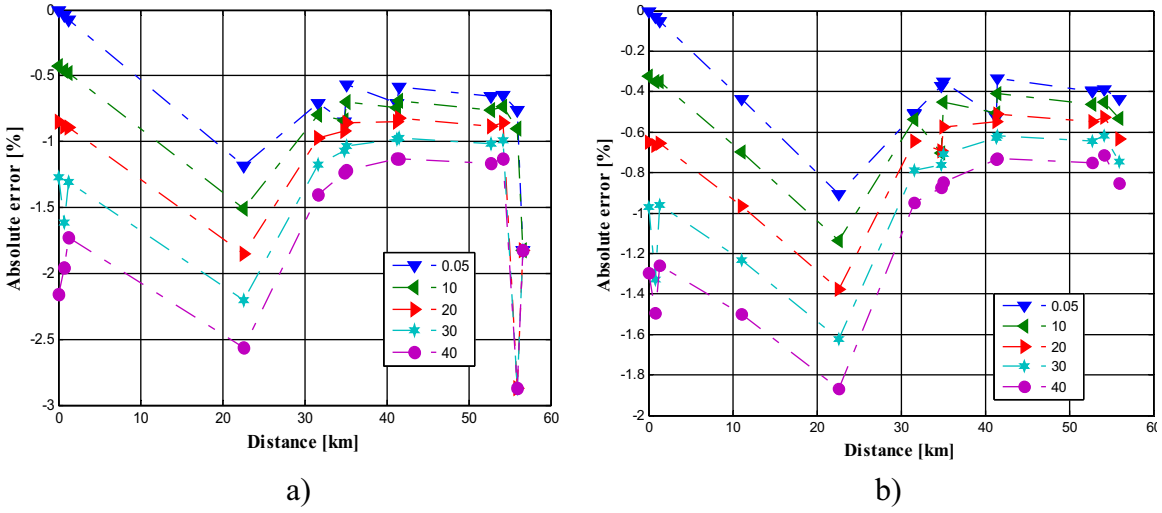

Fig. 6. Performance in case of single-phase to ground faults under rated conditions and (a) DG penetration level of 10%, and (b) DG penetration level of 35%.

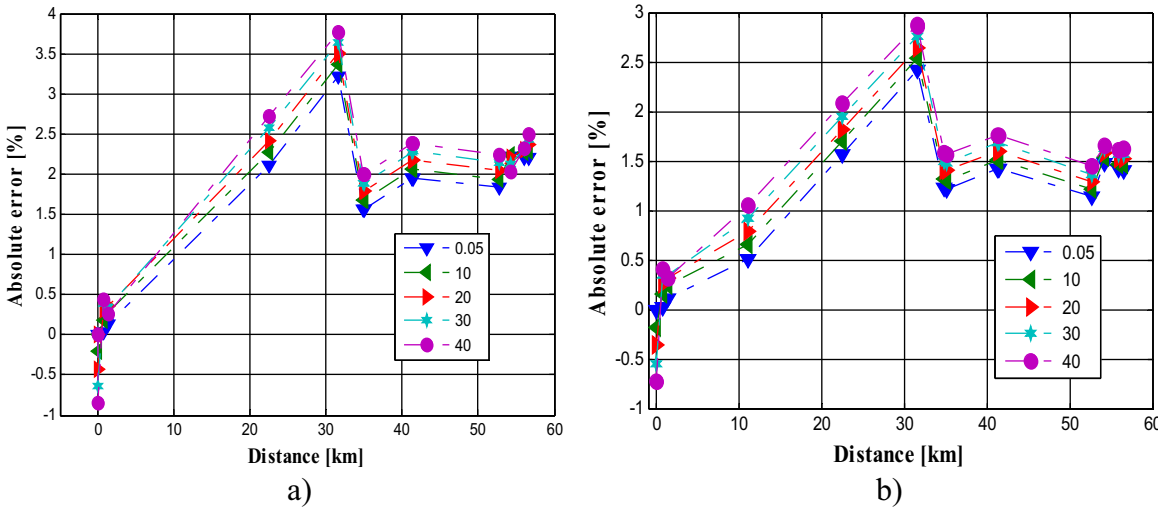

Fig. 7. Performance in case of phase-to-phase to ground faults under rated conditions and (a) DG penetration level of 10%, and (b) DG penetration level of 35%.

Please cite this article in press as: C. Grajales-Espinal, et al., Advanced fault location strategy for modern power distribution systems based on phase and sequence components and the minimum fault reactance concept, Electr. Power Syst. Res. (2016), http://dx.doi.org/10.1016/j.epsr.2016.04.008

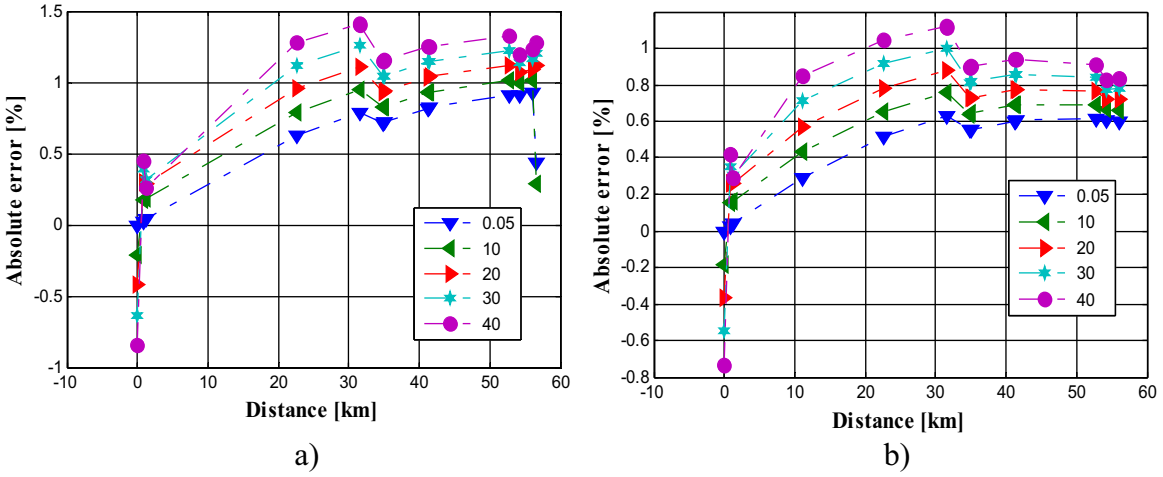

Fig. 8. Performance in case of three-phase faults under rated conditions and (a) DG penetration level of 10%, and (b) DG penetration level of 35%.

considering variations in all loads of the test power system and the DG size. The obtained results are shown in Fig. 9.

Comparing the obtained results to the performance of the method tested under rated conditions, Fig. 9a for single-phase faults depicts how the estimation error increases when load variations are considered. However, this increase is not significant compared to the reference case, as the error differences are lower than 1%. Errors are around the base case and it demonstrates the robustness of the proposed methodology to deal with variations in the operating condition.

As in the case of single-phase to ground fault case, for phase-to-phase faults in the Fig. 9b, the proposed variations have a direct

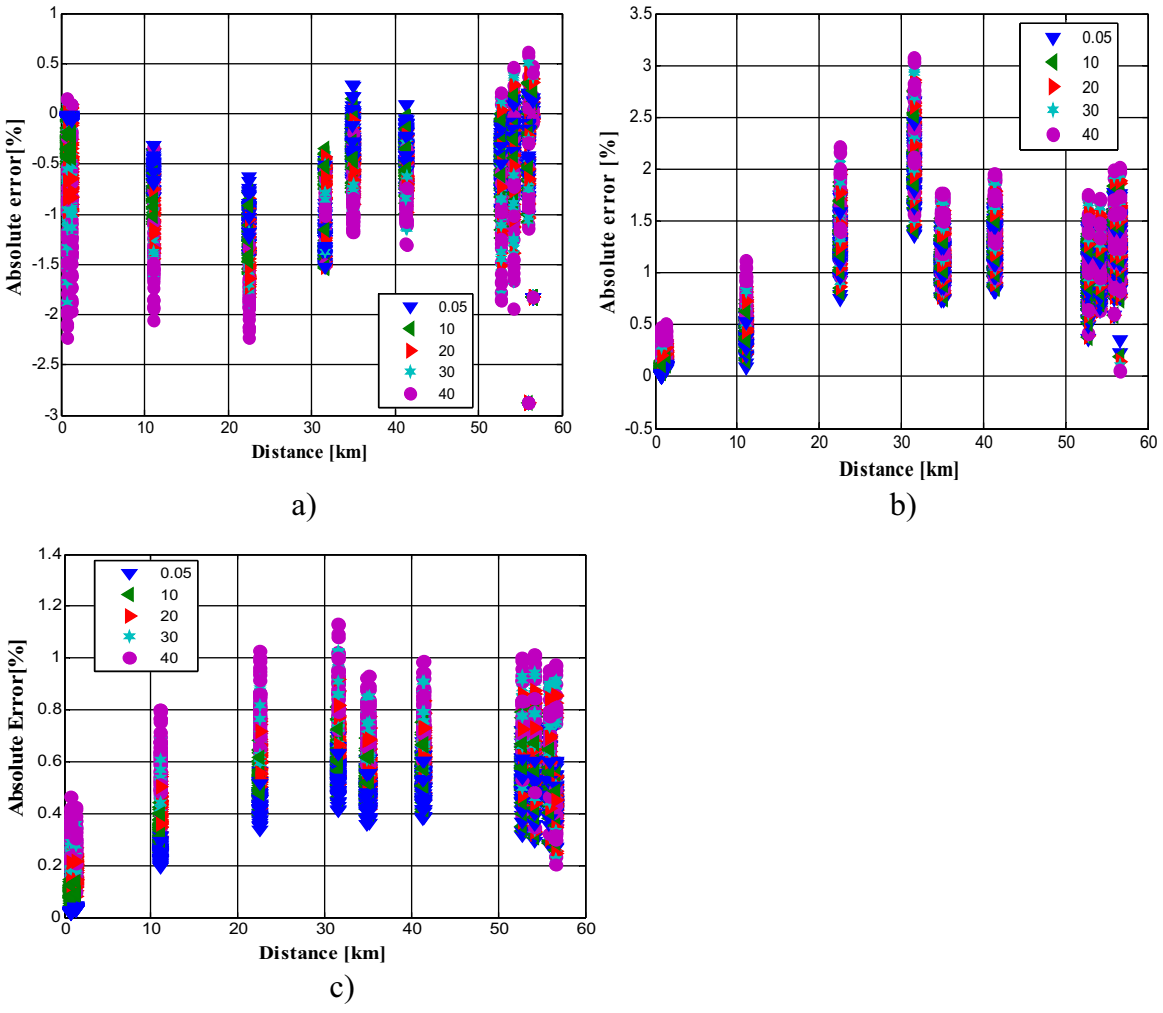

Fig. 9. Performance curves considering several operational conditions in the case of (a) single-phase to ground, (b) phase-to-phase, and (c) three-phase faults.

Please cite this article in press as: C. Grajales-Espinal, et al., Advanced fault location strategy for modern power distribution systems based on phase and sequence components and the minimum fault reactance concept, Electr. Power Syst. Res. (2016), http://dx.doi.org/10.1016/j.epsr.2016.04.008

influence on the fault distance estimation. Nevertheless, due to the load compensation strategy included in the proposed methodology, the error in variation is not significant.

For three-phase faults, the locator performance is similar to that obtained in the case of single-phase to ground and phase-to-phase faults. As in the previous cases, the algorithm suits well for low impedance faults. Additionally, the estimation errors in all of the cases are at the interval from −2.5% to 3.5%, showing an adequate performance of the proposed approach, even in the case of variation in the operating conditions.

Finally, the average time to locate a fault on the IEEE 34 node power system is 59.2 ms. This time was calculated for faults simulated along the main feeder and this performance allows the fast fault location, before the Reclosers changes the feeder topology (around 500 ms approx.). The tests were carried out on an Intel i2 2.66-GHz personal computer with 4 GB RAM.

5. Conclusions

Fault location in power distribution systems leads to an improvement of the continuity indexes; however, the presence of DG forces the reformulation of most of the previous proposed strategies. This paper presents a robust method for fault location in power distribution systems with distributed generation, which only requires voltage and current measurements at the main substation and at the distributed generator substations, to estimate the distance to the faulted node. The proposed method does not require the explicit fault type identification when faults occur is a non-radial zone, which constitutes a remarkable advantage and eliminates errors caused by an inadequate fault identification algorithm.

The obtained results validate the robustness of the proposed method, even in the case of uncertainties caused by realistic load variations and different distributed generation scenarios. Finally, the presented technique helps to solve the fault location problem in real distribution systems with distributed generation, leading to an improvement of the power continuity indexes.

Acknowledgements

This research was supported by the Universidad Tecnológica de Pereira, (Colombia) and COLCIENCIAS, under the project “Desarrollo de localizadores robustos de fallas paralelas de baja impedancia para sistemas de distribución de energía eléctrica LOFADIS 2012”, contract number 0977-2012.

References

[1] F.M. Nuroglu, A.B. Arsoy, Voltage profile and short circuit analysis in distribution systems with DG, in: IEEE Electric Power Conference, 2008, pp. 6–7.
[2] C. Dai, Y. Baghzouz, On the voltage profile of distribution feeders with distributed generation, IEEE Power Eng. Soc. Gen. Meet. 2 (1140) (2003) 13–17.
[3] H. Falaghi, M. Haghifam, Distributed generation impacts on electric distribution systems reliability: sensitivity analysis, in: The International Conference on Computer as a Tool, Nov. 2005, pp. 21–24.
[4] S.M. Brahma, A.A. Girgis, Development of adaptive protection scheme for distribution systems with high penetration of distributed generation, IEEE Trans. Power Del. 19 (1) (2004), pp. 56 and 63.
[5] J. Mora-Flórez, J. Meléndez, G. Carrillo-Caicedo, Comparison of impedance based fault location methods for power distribution systems, Electric Power Syst. Res. 78 (2008) 657–666.
[6] A. Bretas, R. Salim, Fault location in unbalanced DG systems using the positive sequence apparent impedance, in: IEEE PES Transmission and Distribution: Latin America Conference and Exposition, 2006, pp. 1–6.
[7] S.B. Karajgi, G.D. Kamalapur, Fault location estimation in power distribution systems with high penetration of distributed generation, Int. J. Comp. Elect. Eng. 4 (5) (2012).
[8] S.A.M. Javadian, A.M. Nasrabadi, M.R. Haghifam, Determining fault’s type and accurate location in distribution systems with DG using MLP neural networks, in: IEEE International Conference on Clean Electrical Power, 2009, pp. 284–289.
[9] S. Jamali, V. Talavat, Dynamic fault location method for distribution networks with distributed generation, Elect. Eng. 92 (3) (2010) 119–127.
[10] J.U.N. Nunes, A.S. Bretas, A impedance-based fault location technique for unbalanced distributed generation systems, 2011 IEEE PES Trondheim PowerTech 1 (7) (2011) 19–23.
[11] A. Bedoya-Cadena, C. Orozco-Henao, J. Mora-Florez, Single-phase to ground fault locator for distribution systems with distributed generation, in: IEEE PES Transmission and Distribution: Latin America Conference and Exposition, 2012, pp. 3–5.
[12] J.U.N. Nunes, A.S. Bretas, Impedance-based fault location formulation for unbalanced primary distribution systems with distributed generation, Int. Conf. Power Syst. Technol. 1 (7) (2010) 24–28.
[13] R.H. Salim, K.C. Salim, A.S. Bretas, Further improvements on impedance-based fault location for power distribution systems, IET Gen. Transm. Distrib. 5 (2011) 467–478.
[14] S. Lotfifard, M. Kezunovic, M.J.A. Mousavi, Systematic approach for ranking distribution systems fault location algorithms and eliminating false estimates, IEEE Trans. Power Del. 28 (1) (2012) 285–293.
[15] Y. Liao, Generalized fault-location methods for overhead electric distribution systems, IEEE Trans. Power Del. 26 (1) (2010) 53–64.
[16] J. Ren, S.S. Venkata, E. Sortomme, An accurate synchrophasor based fault location method for emerging distribution systems, IEEE Trans. Power Del. 29 (1) (2014) 297–298.
[17] P. Anderson, Analysis of Faulted Power Systems, Wiley–IEEE Press, 1995.
[18] J. Mora-Florez, A. Bedoya, R. Orozco, Fault location considering load uncertainty and distributed generation in power distribution systems, IET Gen. Transm. Distrib. 9 (3) (2015) 287–295.
[19] R. Das, Determining the locations of faults in distribution systems (Doctoral thesis), University of Saskatchewan, Canada, 1998.
[20] G. Morales-España, J. Mora-Flórez, H. Vargas, Fault location method based on the determination of the minimum fault reactance for uncertainty loaded and unbalanced power distribution systems, in: IEEE PES Transmission and Distribution: Latin America Conference and Exposition, 2010, pp. 803–809.
[21] Radial Test Feeder, IEEE Distribution System Analysis Subcommittee, available from: http://ewh.ieee.org/soc/pes/dsacom/testfeeders/index.html.
[22] J. Dagenhart, The 40-ohms ground-fault phenomenon, IEEE Trans. Ind. Appl. 36 (1.) (2000) 30–32.
[23] N. Alzate-Gonzalez, J. Mora-Florez, S. Perez-Londono, Methodology and software for sensitivity analysis of fault locators, in: IEEE PES Transmission and Distribution: Latin America Conference and Exposition, 2014, pp. 1–6.

Please cite this article in press as: C. Grajales-Espinal, et al., Advanced fault location strategy for modern power distribution systems based on phase and sequence components and the minimum fault reactance concept, Electr. Power Syst. Res. (2016), http://dx.doi.org/10.1016/j.epsr.2016.04.008